



## Letter

Effect of La<sub>2</sub>O<sub>3</sub> on microstructures and laser properties of Nd:YAG ceramicsWenbin Liu<sup>a,b</sup>, Jiang Li<sup>b</sup>, Benxue Jiang<sup>b</sup>, Di Zhang<sup>a</sup>, Yubai Pan<sup>b,\*</sup><sup>a</sup> State Key Laboratory of Metal Matrix Composites, Shanghai Jiao Tong University, Shanghai 200240, PR China<sup>b</sup> State Key Laboratory of Transparent Opto-functional Inorganic Materials, Shanghai Institute of Ceramics, Chinese Academy of Sciences, Shanghai 200050, PR China

## ARTICLE INFO

## Article history:

Received 21 June 2011

Received in revised form

14 September 2011

Accepted 14 September 2011

Available online 19 September 2011

## Keywords:

La<sub>2</sub>O<sub>3</sub>

Nd:YAG

Ceramics

Microstructures

Optical materials and properties

## ABSTRACT

Transparent 1.0 at.% Nd:YAG ceramics were fabricated by vacuum sintering technology using commercial  $\alpha$ -Al<sub>2</sub>O<sub>3</sub>, Y<sub>2</sub>O<sub>3</sub> and Nd<sub>2</sub>O<sub>3</sub> powders as raw materials. Influence of La<sub>2</sub>O<sub>3</sub> additions (0–1.2 wt%) on microstructures and optical properties of Nd:YAG ceramics was investigated. The results indicate that the optical properties of Nd:YAG ceramics with 0.4 wt% La<sub>2</sub>O<sub>3</sub> are superior than those of undoped-Nd:YAG ceramics. When the amount of La<sub>2</sub>O<sub>3</sub> is 0.8 wt%, the specimen has the highest transmittance in the region from 400 nm to 1100 nm. No pores or other defects are found in or between the grains. However, residual inclusions along grain boundaries and pores are easily generated by adding excessive La<sub>2</sub>O<sub>3</sub> (1.2 wt%). The Nd:YAG ceramics are pumped by a diode laser to study the laser properties. The slope efficiency and threshold of Nd:YAG ceramics with optimum addition of La<sub>2</sub>O<sub>3</sub> (0.8 wt%) are 41.1% and 2.9 W, respectively, which are the best laser oscillation results among all the specimens.

© 2011 Elsevier B.V. All rights reserved.

## 1. Introduction

As a solid-state laser material, neodymium-doped yttrium aluminum garnet (Nd:YAG) single crystals fabricated by the Czochralski method has been widely used as solid in laser systems for industrial, medical, scientific, and military purposes [1,2]. However, the growing technique for Nd:YAG single crystals requires great skills, the requirement of expensive Ir crucibles and the difficulty in growing large size crystal with high Nd<sup>3+</sup> doping concentration has prevented their further applications [3]. In 1995, Ikesue et al. fabricated transparent Nd:YAG ceramics with the required optical properties for laser applications [4,5]. Since then, Nd:YAG transparent ceramics have attracted much attention because the optical properties have been improved greatly and the highly efficient laser oscillations have been obtained.

Compared with single crystals, Nd:YAG ceramics have several advantages, such as lower cost, large size, high concentrations doping, multifunctional composite structure, and so on [6,7]. Thus, tremendous efforts have been made to develop synthesis methods for YAG ceramics [8–15]. In order to fabricate high-transparency Nd:YAG ceramics, pores should be eliminated as much as possible [16]. If the grain size is too large, it is difficult to remove the residual pores because there are less grain boundaries for pores release. So it is better to find a way to control the grain growth rate. Some reports [17,18] show that the abnormal grain growth can be

inhibited by adding sintering aids such as MgO and SiO<sub>2</sub>. Unfortunately, a few residual pores are still observed, the optical qualities of Nd:YAG ceramics are a little inferior to those of single crystals due to the residual pores in the ceramics act as optical scattering centers [5]. Lanthana (La<sub>2</sub>O<sub>3</sub>) is a sintering aid which has been successfully applied to fabricate Y<sub>2</sub>O<sub>3</sub> ceramics [19,20]. The addition of La<sub>2</sub>O<sub>3</sub> is helpful to promote desiccation and decrease sintering temperature, and then decrease the grain boundary diffusion coefficient. The La<sub>2</sub>O<sub>3</sub>-doped Y<sub>2</sub>O<sub>3</sub> ceramics display pore-free microstructures and high optical qualities [21]. Therefore, it is possible to improve the optical properties of Nd:YAG ceramics by doping La<sub>2</sub>O<sub>3</sub>. In this work, Nd:YAG ceramics were fabricated by solid-state reaction and vacuum sintering method using La<sub>2</sub>O<sub>3</sub> as a sintering aid. The effect of various amount of La<sub>2</sub>O<sub>3</sub> on the microstructures and optical properties of Nd:YAG ceramics was investigated.

## 2. Experimental procedures

## 2.1. Fabrication of Nd:YAG ceramics

High-purity powders of  $\alpha$ -Al<sub>2</sub>O<sub>3</sub> ( $\geq 99.99\%$ , Alfa Aesar Company, USA), Y<sub>2</sub>O<sub>3</sub> ( $\geq 99.99\%$ , Alfa Aesar Company, USA), Nd<sub>2</sub>O<sub>3</sub> ( $\geq 99.99\%$ , Alfa Aesar Company, USA) and La<sub>2</sub>O<sub>3</sub> ( $\geq 99.99\%$ , Alfa Aesar Company, USA) were used as starting materials. These powders were mixed according to the stoichiometric Y<sub>2.97</sub>Nd<sub>0.03</sub>Al<sub>5</sub>O<sub>12</sub> with different contents of La<sub>2</sub>O<sub>3</sub> and ball-milled with the high-purity Al<sub>2</sub>O<sub>3</sub> balls for 10 h in ethanol using tetraethylorthosilicate (TEOS) as sintering aid. The mass fractions of La<sub>2</sub>O<sub>3</sub> in the resultant Nd:YAG ceramics were controlled to 0 wt%, 0.4 wt%, 0.8 wt% and 1.2 wt%, respectively. The mixture of the powders was dried and sieved through a 200-mesh screen. After removing the organic component by calcining at 800 °C for 4 h, the powders were dry-pressed under 20 MPa into  $\varnothing$  30 mm  $\times$  7 mm disks and finally cold-isostatically pressed under 250 MPa. Green compacts were sintered at 1730 °C for 20 h under vacuum ( $1.0 \times 10^{-3}$  Pa), after that, the pellets were annealed

\* Corresponding author. Tel.: +86 21 52412820; fax: +86 21 52413903.

E-mail address: [ybpan@mail.sic.ac.cn](mailto:ybpan@mail.sic.ac.cn) (Y. Pan).

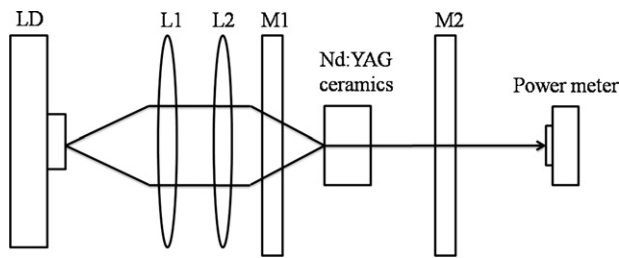


Fig. 1. Schematic diagram of the laser experimental setup.

at 1450 °C for 20 h in air and mirror polished on both surfaces. The Nd:YAG ceramics were obtained, and named as specimens A, B, C and D, respectively.

The microstructures of specimens were observed by electron probe micro-analyzer (EPMA, Model JXA-8100, JEOL, Japan). The transmittance spectra were measured with a spectrophotometer (Model U-2800, Hitachi, Japan). The photoluminescence spectra were measured at room temperature by spectrofluorometer (Model Fluorolog-3, Jobin Yvon, France), with an 808 nm diode laser used as pump source.

## 2.2. Laser experiment

The experimental setup for oscillation is shown in Fig. 1. The Nd:YAG ceramics are processed into shape of 3 mm × 3 mm × 6 mm and mirror polished on both surfaces and coated on two parallel end facets. The input facets are high transmittance coated at 808 and 1064 nm, while the output facets are antireflection coated at 808 nm. A 15 W ring-shaped laser diode (LD) with the emission wavelength of 808 nm is used as pump source. The laser cavity consists of two flat mirrors (M1 and M2), where M1 is antireflection-coated at 808 nm and high-reflection at 1064 nm as the input coupler (IC), and M2 is output coupler (OC) with transmittance of 5% at 1064 nm.

## 3. Results and discussion

Fig. 2 shows a photograph of mirror polished Nd:YAG ceramics sintered at 1730 °C for 20 h after annealing at 1450 °C for 10 h. All specimens exhibit good transparency. Words behind it can be read clearly. As can be seen from Fig. 3, the transmittances of specimens A, B, C and D are all above 82% at the lasing wavelength of 1064 nm. According to the Rayleigh's equation, the scattering

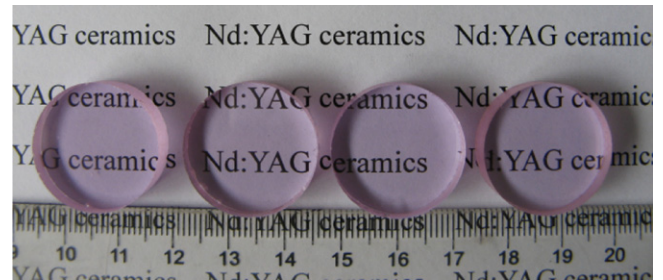


Fig. 2. Photograph of specimens (5 mm thickness) with various contents of  $\text{La}_2\text{O}_3$ , (a) without  $\text{La}_2\text{O}_3$ , (b) 0.4 wt%, (c) 0.8 wt%, and (d) 1.2 wt%.

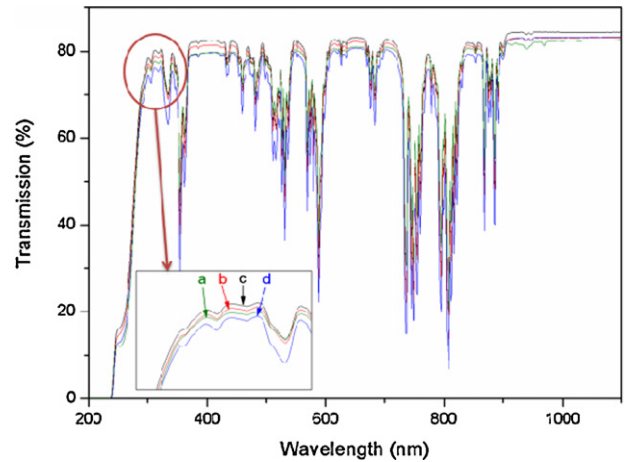


Fig. 3. Optical transmissions of specimens with various contents of  $\text{La}_2\text{O}_3$ , (a) without  $\text{La}_2\text{O}_3$ , (b) 0.4 wt%, (c) 0.8 wt%, and (d) 1.2 wt%.

intensity increases with decreasing of wavelength [22]. The optical transmittance is 79.7% for specimen A, 81.4% for specimen B, 82.5% for specimen C and 79.6% for specimen D at 400 nm, respectively. The transmittance of specimen C is the best of all in the region from

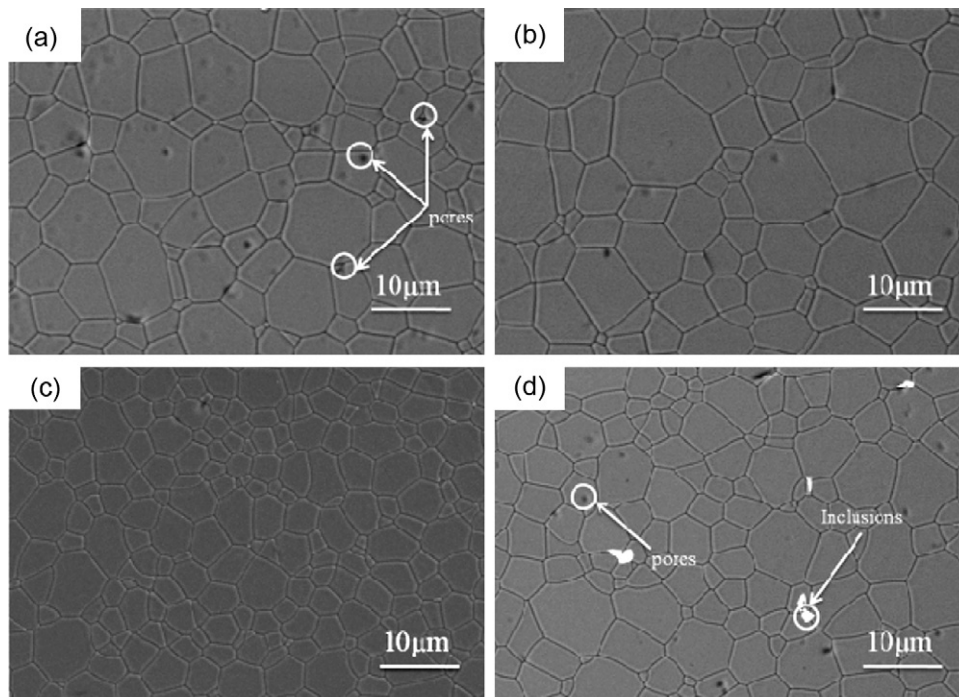


Fig. 4. SEM of specimens with various contents of  $\text{La}_2\text{O}_3$ , (a) without  $\text{La}_2\text{O}_3$ , (b) 0.4 wt%, (c) 0.8 wt%, and (d) 1.2 wt%.

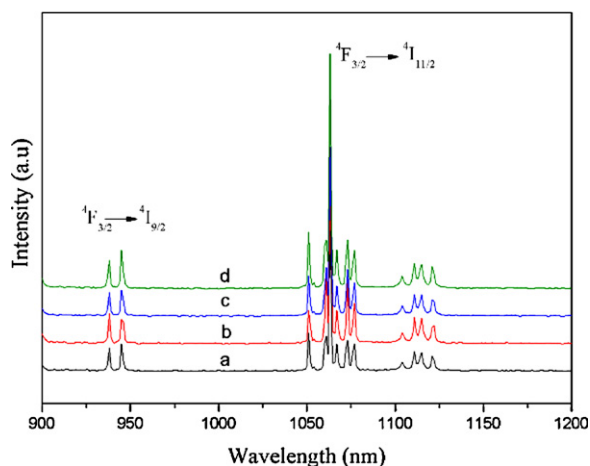


Fig. 5. Photoluminescence spectra of specimens with various contents of  $\text{La}_2\text{O}_3$ , (a) without  $\text{La}_2\text{O}_3$ , (b) 0.4 wt%, (c) 0.8 wt%, and (d) 1.2 wt%.

400 nm to 1100 nm, which is very close to that of single crystal [4]. The result indicates that the optimum addition of (0.8 wt%)  $\text{La}_2\text{O}_3$  will help to improve the optical properties of Nd:YAG ceramics.

In order to detect the main reason for decreasing of the transmittance of specimens at 400 nm, the micrographs of specimens with different quantities of  $\text{La}_2\text{O}_3$  are observed by EPMA (Fig. 4). If there is no  $\text{La}_2\text{O}_3$  as a sintering aid, a few pores are observed both at the grain boundaries and inner grains (Fig. 4(a)). For  $\text{La}_2\text{O}_3$  dopant of 0.4 wt%, the amount of pores decreases in the Nd:YAG ceramics (Fig. 4(b)), and for 0.8 wt%, no pores or other defects can be found (Fig. 4(c)). The average grain size of specimen C with pore-free microstructures is smaller than that of specimen B. It is because that  $\text{La}_2\text{O}_3$  is prone to segregate at the grain boundaries, which will decrease the grain growth kinetics. As the grain growth rate is slower than the pore diffusion rate, pores can be removed easily from the specimen C. However, as can be seen from Fig. 4(d), some residual inclusions and apparent pores are formed at grain boundaries because of the addition of excessive  $\text{La}_2\text{O}_3$  (1.2 wt%). This is detrimental to the optical properties of Nd:YAG ceramics (Fig. 3). Consequently, the addition of  $\text{La}_2\text{O}_3$  should be accurately controlled.

The photoluminescence spectra of Nd:YAG ceramics with various  $\text{La}_2\text{O}_3$  contents are shown in Fig. 5. From 900 nm to 1200 nm, there are two emission bands centered at 946 nm and 1064 nm, which are corresponding to the transition from  $^4F_{3/2} \rightarrow ^4I_{9/2}$  and  $^4F_{3/2} \rightarrow ^4I_{11/2}$  of  $\text{Nd}^{3+}$  ions, respectively. No obvious wavelength redshift has been observed with increasing concentrations of the  $\text{La}_2\text{O}_3$ . The fluorescent line widths for Nd:YAG ceramics with 0 wt%, 0.4 wt%, 0.8 wt% and 1.2 wt%  $\text{La}_2\text{O}_3$  are almost identical. It means the addition of small amount  $\text{La}_2\text{O}_3$  has no effect on the spectral properties of Nd:YAG ceramics despite of the slight lattice distortion caused by its doping.

Fig. 6 shows laser output versus pump power for Nd:YAG ceramics at 1064 nm. With 13.6 W of maximum absorbed pump power, laser output power of specimens B and C are 3.3 W and 4.4 W respectively. The threshold for both specimens B and C is 2.9 W. The slope efficiency of specimen B is 30.8%, which is 10.3% lower than that of specimen C (41.1%). The laser output of specimens A and D cannot be achieved, the main reason is that there are some residual pores or other defects in the two specimens (Fig. 4(a and d)). Compared with the previous reports, it is also found that the laser properties of specimen C are inferior to those of single crystals [5]. These may attribute to losses mainly caused by grain boundaries and some residual defects (cannot be detected) in the Nd:YAG

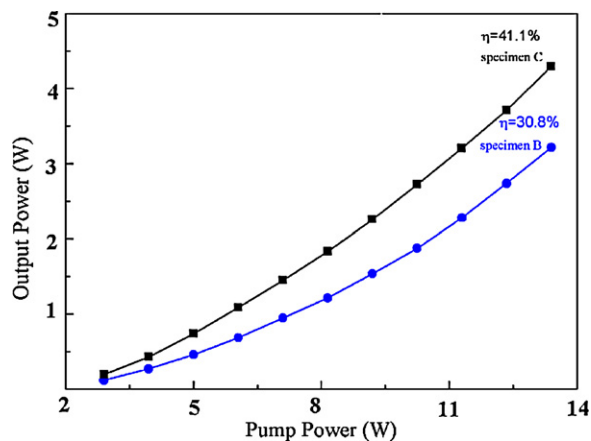


Fig. 6. Laser output at 1064 nm versus pump power.

ceramics. The detailed relation between microstructures and scattering loss will be further studied.

#### 4. Conclusions

Transparent Nd:YAG ceramics were fabricated by solid-state reaction and vacuum sintering using  $\text{La}_2\text{O}_3$  as sintering aid. The small amount of  $\text{La}_2\text{O}_3$  helps to control abnormal grain growth, and refine the microstructures of Nd:YAG ceramics. The maximum refinement in microstructures is obtained with the optimum addition (0.8 wt%) of  $\text{La}_2\text{O}_3$ . The specimen C with average grain size of about 8  $\mu\text{m}$  has a fine microstructure. No pores or other defects appear in or between the grains. The optical properties of specimen C are superior to those of the other three specimens in the region from 400 nm to 1100 nm. The slope efficiency and threshold for specimen C are 41.1% and 2.9 W, respectively, which are the best laser oscillation results in all the specimens.

#### Acknowledgements

This work was supported by the Innovation Technology Funding of Shanghai Institute of Ceramics (no. Y04ZC3130G), NSFC (no. 50990300), the Major Basic Research Programs of Shanghai (no. 07DJ14001) and the Natural Science Foundation of Shanghai (no. 10ZR1433900).

#### References

- [1] A.A. Kaminskii, *Laser Photon. Rev.* 1 (2007) 93–177.
- [2] K. Ueda, N. Uehara, *Rev. Laser Eng.* 21 (1993) 859–872.
- [3] M. Katsurayama, Y. Anzai, A. Sugiyama, M. Koike, Y. Kato, *J. Cryst. Growth* 229 (2001) 193–198.
- [4] A. Ikesue, I. Furusato, K. Kamata, *J. Am. Ceram. Soc.* 78 (1995) 225–228.
- [5] A. Ikesue, T. Kinoshita, K. Kamata, K. Yoshida, *J. Am. Ceram. Soc.* 78 (1995) 1033–1040.
- [6] R. Feldman, Y. Golan, Z. Burshtein, S. Jackel, I. Moshe, A. Meir, Y. Lumer, Y. Shimony, *Opt. Mater.* 33 (2011) 695–701.
- [7] T. Taira, *C. R. Physique* 8 (2007) 138–152.
- [8] W.B. Liu, W.X. Zhang, J. Li, H.M. Kou, Y.Q. Shen, L. Wang, Y. Shi, *J. Alloys Compd.* 503 (2010) 525–528.
- [9] Y.K. Li, S.M. Zhou, H. Lin, X.R. Hou, W.J. Li, H. Teng, T.T. Ji, *J. Alloys Compd.* 502 (2010) 225–230.
- [10] W.B. Liu, W.X. Zhang, J. Li, H.M. Kou, D. Zhang, Y.B. Pan, *J. Eur. Ceram. Soc.* 31 (2011) 653–657.
- [11] L. Yang, T.C. Lu, H. Xu, N. Wei, *J. Alloys Compd.* 484 (2009) 449–451.
- [12] G.F. Li, Q. Cao, Z.M. Li, Y.X. Huang, Y.G. Wei, J.Y. Shi, *J. Alloys Compd.* 485 (2009) 561–564.
- [13] Z.G. Wu, X.D. Zhang, W. He, Y.W. Du, N.T. Jia, P.C. Liu, F.Q. Bu, *J. Alloys Compd.* 472 (2009) 576–580.
- [14] H. Yang, X.P. Qin, J. Zhang, S.W. Wang, J. Ma, L.X. Wang, Q.T. Zhang, *J. Alloys Compd.* 509 (2011) 5274–5279.
- [15] M.L. Saladino, G. Nasillo, D.C. Martino, E. Caponetti, *J. Alloys Compd.* 491 (2010) 737–741.

- [16] D.L. Jiang, *J. Inorg. Mater.* 24 (2009) 873–881.
- [17] X.P. Qin, H. Yang, G.H. Zhou, D.W. Luo, J. Zhang, S.W. Wang, J. Ma, *Mater. Res. Bull.* 46 (2011) 170–174.
- [18] Y.K. Li, S.M. Zhou, H. Lin, X.R. Hou, W.J. Li, H. Teng, T.T. Jia, *J. Alloys Compd.* 502 (2010) 225–230.
- [19] X.M. Hu, Q.H. Yang, C.G. Dou, J. Xu, H.X. Zhou, *Opt. Mater.* 30 (2008) 1583–1586.
- [20] Q.H. Yang, J. Xu, L.B. Su, H.W. Zhang, *Acta Phys. Sin.* 64 (2006) 1207–1210.
- [21] Y.H. Huang, D.L. Jiang, J.X. Zhang, Q.L. Lin, *J. Am. Ceram. Soc.* 92 (2009) 2883–2887.
- [22] A. Ikesue, K. Kamata, T. Yamamoto, I. Yamaga, *J. Am. Ceram. Soc.* 80 (1997) 1517–1522.